Theoretical and experimental studies of the electronic states of the diatomic cation Cl_2^{2+}

P. G. Fournier, J. Fournier, and F. Salama
Spectroscopie de Translation et Dynamiques des Interactions Moléculaires, Université Paris—Sud, 91404 Orsay, France

D. Stärk and S. D. Peyerimhoff
Lehrstuhl für Theoretische Chemie, Universität Bonn, Wegelstrasse 12, D-5300 Bonn 1, West Germany

J. H. D. Eland
Physical Chemistry Laboratory, South Parks Road, Oxford, United Kingdom
(Received 14 February 1986)

Energies of the singlet states of the doubly charged chlorine cation have been determined experimentally by the technique of double charge transfer, and are compared with the results of multireference single- and double-excitation configuration-interaction calculations. The good agreement obtained permits an assignment of all the peaks in the experimental spectrum, and confirms the accuracy of these calculations, which also predict energies of the unobserved triplet states. The experimental spectrum due to single charge transfer is explained in terms of the photoelectron spectrum.

INTRODUCTION

The high density of electronic states of doubly charged molecular cations makes accurate calculations of their potential energy curves difficult,[1] while only fragmentary information has hitherto been available from extant experimental methods. In Auger spectroscopy,[2] the doubly charged ion in singlet states is reached from a hole state of the singly charged precursor. In the photoion-photoion coincidence technique, dissociative doubly charged ions formed by photon impact are detected by a mass-spectrometric apparatus.[3] The energies of the lowest-energy accessible states can be deduced from the thresholds for fragmentation into cation pairs, or for formation of metastable doubly charged species. In charge-stripping experiments, doubly charged ions are formed in a two-step process. Primary ions (A^+) collide with a target M and measurement of the translational energy distribution of the resultant long-lived A^{2+} allows one to determine the energy defect for the $A^+ \rightarrow A^{2+}$ transition.[4] The double charge-transfer technique described here presents more accurate information complementary to that from the above techniques. It permits the determination of the energies and Franck-Condon zone widths in the vertical double ionization even if the populated states are unstable with respect to dissociation.[5] Energy levels of doubly charged states of rare-gas target and diatomic molecules O_2, N_2, and NO have been studied earlier[6] and an attempt has been made from the theoretical point of view to determine the symmetry and electron-spin selection rules in such processes.[6,7] It has also been demonstrated for H_2 that the process obeys the Franck-Condon principle.[8]

We have extended these studies to the case of the chlorine molecule. Very few experimental results are available on Cl_2^{2+}, and we present in this work the first detailed study of this dication. It turns out to be a good test case for the selection rules governing double charge transfer to homonuclear diatomics and also for theoretical calculations. The first stable doubly charged state has previously been located at 32.6 eV by a conventional electron-impact technique.[9] Measurement of the energy release during the decomposition of doubly charged chlorine species in a double mass spectrometer[10] led to the identification of a Cl_2^{2+} metastable state. Its lifetime was estimated to be of the order of 10^{-5} sec and its energy was estimated as 33.2 eV on the assumption that this state decomposes to fragments $Cl^+(^3P_2)+Cl^+(^3P_2)$. The first theoretical study of the Cl_2^{2+} cation was carried out by Hurley *et al.*[11] employing an approach in which the quantum-mechanical virial theorem was used to derive potential energy curves for the doubly ionized ion from the self-consistent-field (SCF) type curve of the related neutral molecule. They obtained good agreement with experimental appearance potentials but pointed out that the test of the theory was vitiated by uncertainties in the experimental values. In the case of Cl_2 the predicted appearance potential was 32.57 eV. As the theoretical methods have improved considerably since this early calculation we decided to undertake a large-scale multireference single- and double-excitation configuration-interaction (MRD-CI) study of the Cl_2^{2+} states parallel to the experimental work.

EXPERIMENTAL PROCEDURE

The double charge-transfer technique involves measurement of the translational energy of H^- ions arising from the acquisition of two electrons by incident protons impinging on a gaseous target (M). This can happen either in a single-step process,

$$H^+ + M \rightarrow H^- + M^{2+} \quad \text{(process I)},$$

where the two electrons are extracted from a single target molecule M which becomes a doubly charged ion M^{2+} or

in two successive single charge exchanges,

$$H^+ + M \rightarrow M^+(y) + H \quad \text{(process IIa)},$$

$$H + M \rightarrow M^+(z) + H^- \quad \text{(process IIb)},$$

where the M^+ species produced in each collision may not be in the same electronic state. For process I, the value of the double ionization potential is determined using the following relation:

$$I^{2+} = -(E - E_0) - T_m - E(H^-),$$

where E_0 is the initial kinetic energy of the protons, E is the measured kinetic energy of the H^- ions, $E(H^-)$ is the energy required to produce H^- in its ground state from H^+, and T_m is the recoil velocity of M^{2+}. The single ionization potentials of M are given by process II:

$$I^+(M(y)) + I^+(M(z)) = -(E - E_0) - T_m(y) - T_m(z) - E(H^-),$$

where $I^+(M(y))$ and $I^+(M(z))$ are the ionization energies required to produce M^+ in the states y and z. $T_m(y)$ and $T_m(z)$ are the recoil energies of $M(y)$ and $M(z)$. Illustration of processes I and II are given in Fig. 1.

The flight time from the collision chamber to the detector is too long (larger than 10^{-6} sec) for the excited $2p^2(^3P)$ state of H^-, which has a lifetime of 1.73×10^{-9} sec,[12] to be detected. $E(H^-) = -(13.56 + 0.79) = -14.35$ eV.

The apparatus is based on a double mass spectrometer equipped with a modified plasma ion source[5] in which the H^+ ions are formed by electron impact on H_2. In order to obtain protons having a small kinetic energy distribution the ion source was tuned at low electron energy (40 eV), so the main formation mechanism is electronic transition to the dissociative part of the ground state of $H_2^+(1s\sigma_g)$.

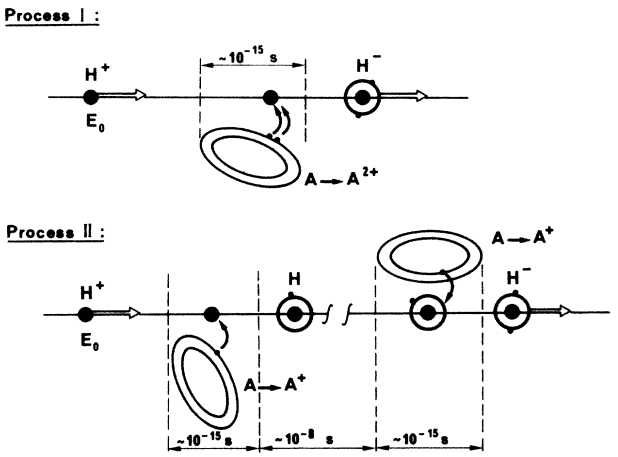

FIG. 1. Illustration of the processes leading to the H^- formation. The upper part shows double charge transfer where during the collision time estimated at 10^{-15} sec the two electrons jump simultaneously onto the H^+ projectile. The lower part shows the two-step formation of H^- by the charge transfer and ion pair formation. The time between two collisions is estimated at half the traveling time through the collision chamber.

The high pressure of H_2 then thermalizes the emitted protons. 3-keV primary ions are mass analyzed by a Wien filter having a resolution of 300. The beam is angularly defined by two 30-μm-diam holes 30 cm apart, before being led into an electrically floating collision chamber of 10 cm length, where the target gas is introduced. The scattered or secondary beam is also angularly selected using a hole of 30 μm, 20 cm from the collision chamber, and can be deflected across the collimating slit by a small transverse electric field. This permits the detection of the H ions in an almost-zero scattering angle. In such conditions, the recoil energies of the target species [T_m, $T_m(y)$, $T_m(z)$] are negligible.

The secondary ions are energy selected by a 127° electrostatic analyzer with a resolving power of 4000 and are detected by a tubular multiplier. We remove the signal from collisions with residual gas in other parts of the apparatus by applying a potential V to the collision chamber, so the H^- ions formed in the collisions are, respectively, unaffected or shifted by the values $2V$ depending on where the collisions happen. In order to avoid focusing and defocusing effects low voltage (100 V) must be used. Pressures in the target region and the main vacuum chamber were measured using a cold-cathode gauge and an ionization gauge, respectively.

CALCULATIONS

The calculations are all of the multireference single- and double-excitation configuration-interaction (MRD-CI) type as described elsewhere.[13,14] All single- and double-excitation configurations relative to the set of reference configurations (which represent the main part of the wave function) are generated and constitute the total MRD-CI space; the number of main or reference configurations (denoted by "x main" in Table I) lies between 7 and 47 depending on the state under discussion and the total MRD-CI spaces range from 95 881 for the Cl_2 ground state to over 10^6 for the various states of Cl_2^{2+} (Table I). From the total MRD-CI space only those excitations which interact heavily with the reference set (to produce an energy lowering of more than 10 μhartrees) are selected to be included in the secular equation (Hamiltonian CI matrix) to be solved explicitly while the effect of all others is perturbatively taken into account via an extrapolation technique;[14] the resulting energy is denoted by E_{MRD}. In this manner the secular equations actually solved are much smaller than the total MRD-CI space and range between 2800 for Cl_2^+ and almost 14 000 for Cl_2^{2+} (Table I). For computational convenience all calculations are carried out in the Abelian subgroup D_{2h} rather than in the $D_{\infty h}$ point group, which possesses degenerate irreducible representations; the correspondence is also indicated in Table I which summarizes all technical details of the calculations. Separate calculations are carried out for the various spin and spatial symmetries but states of the same symmetry are always obtained from the same secular equation (as higher roots, also indicated in Table I). In this case, the configuration selection from the total MRD-CI space is undertaken with respect to all desired states (y roots) of the symmetry under consideration. In

TABLE I. Technical details of the calculations at $R=2.0$ Å. In the standard treatment the range of selected configurations at various values of R is given.

	Symmetry		Standard treatment[a]		Parent MO treatment[b]		Larger basis treatment[b,c]	
System	D_{2h}	$D_{\infty h}$	x main/y root[d]	CI space[e] total/selected	x main/y root[d]	CI space[e] total/selected	x main/y root[d]	CI space[e] total/selected
Cl_2	$^1A_{1g}$	$^1\Sigma_g^+$	8/2	95 881/6400–7000			13/1	511 233/5021
Cl_2^+	$^2B_{1g}$	$^2\Pi_g$	7/1	231 136/2800–3500			10/1	555 264/6485
Cl_2^{2+}	$^1A_{1g}$	$^1\Sigma_g^+,{}^1\Delta_g$	38/4	539 010/10 567–8199	38/4	539 010/11 610	12/2	299 466/5981
	$^1B_{3u}$	$^1\Sigma_u^+,{}^1\Delta_u$	31/2	669 296/7597–4958	33/2	686 411/5637	9/2	240 186/6509
	$^3B_{3u}$	$^3\Sigma_u^+,{}^3\Delta_u$	30/2	1 186 349/9435–8105	30/2	1 186 349/5948	9/2	399 199/6038
	$^3B_{3g}$	$^3\Sigma_g^-$	30/2	1 220 625/9860–5934	30/2	1 220 625/9031	11/2	655 644/10 679
	$^1B_{1g}$	$^1\Pi_g$	42/3	867 391/13 669–9355	42/3	867 391/10 133	11/2	374 357/9271
	$^3B_{1g}$	$^3\Pi_g$	38/2	1 486 844/9545–8473	38/2	1 486 894/9483	11/2	657 227/10 334
	$^1B_{2u}$	$^1\Pi_u$	29/3	618 189/13 208–7271	29/3	618 189/12 446	10/2	368 792/9832
	$^3B_{2u}$	$^3\Pi_u$	32/2	1 279 530/10 599–6335	32/2	1 279 530/9440	10/2	650 862/10 004
	^3A_u	$^3\Sigma_u^-,{}^3\Delta_u$	21/4	890 585/11 420–7529	21/4	890 585/10 369	13/3	995 672/10 282
	^1A_u	$^1\Sigma_u^-,{}^1\Delta_u$	47/3	1 124 484/9895–7528	47/3	1 091 948/9586	13/3	54 994/11 282

[a]Standard treatment, employed for the calculation of the Cl_2^{2+} potential energy curves.
[b]$X\,^3\Sigma_g^-$ MO's for all states of Cl_2^{2+}, $^1\Sigma_g^+$ MO's for Cl_2 and Cl_2^+.
[c]Results obtained from the large AO basis set.
[d]Size of the reference set (x main) and number of states (y roots) for which configuration selection is carried out.
[e]Size of the total generated MRD-CI space and size of the selected subspace for which diagonalization is made.

addition to the MRD-CI, energy which would correspond to the full CI space (higher than double excitations) is also estimated as

$$E_{\text{full}}=E_{\text{MRD}}+\Delta E\ ,$$

whereby the correction is evaluated as

$$\Delta E=(E_{\text{MRD}}-E_{\text{ref}})\left[1-\sum_{\text{ref}}c_0^2\right]\ .$$

In this formula E_{ref} is the energy obtained from the reference set only and $\sum_{\text{ref}}c_0^2$ is the contribution of all reference configurations in the final wave function, which in the present calculations is always around 0.9 or larger.

The atomic-orbital (AO) basis set for the standard Cl_2^{2+} calculations is the same as that employed in the previous treatment of the potential energy curves of the Cl_2 molecule[15] and its positive ion;[16] in fact for computational convenience the molecular-orbital (MO) integral tapes from the prior calculations on Cl_2 have been employed. Hence the AO and MO basis is not made optimal for the chlorine dication but rather results from a standard calculation for the neutral system. This aspect should be kept in mind in evaluating the accuracy of the computed results.

At the Cl_2 ground-state equilibrium geometry two additional calculations have been undertaken. The first one employs the SCF MO's of the $X^3\Sigma_g^-$ Cl_2^{2+} state for all states of the dication, i.e., molecular orbitals which should be somewhat more appropriate than the $X\,^1\Sigma_g^+$ MO's of chlorine employed in the standard calculations. This aspect can also be seen from the somewhat smaller secular equation (Table I) which indicates a more compact wave function. The total SCF energy for the $X\,^3\Sigma_g^-$ state is $-917.778\,52$ hartrees; the corresponding CI energies are $E_{\text{MRD}}=-918.130\,23$ hartrees and $E_{\text{full}}=-918.152\,03$ hartrees.

The second calculation employed a larger AO basis without Rydberg functions. It is based on the $(13s\,9p)$ set of McLean and Chandler[17] contracted to $[8s\,5p]$, augmented by two contracted d functions (exponents 3.5 and 0.8 with contraction coefficients 0.062 76 and 0.241 76, and exponent 0.3) and one f function (exponent 0.7). The most diffuse s and p functions as well as the d and f functions have been optimized for a calculation on HCl^+.[18] Bond polarization functions [$\alpha(s)=1.0$ and $\alpha(p)=0.6$] have also been added so that this AO basis contains a total of 94 contracted Gaussians. As in the previous cases a core of ten MO's corresponding to the K and L shells of chlorine is held doubly occupied and the two MO's with the highest SCF orbital energy are discarded entirely from the calculations leaving a total of 62 MO's among which the 12 valence electrons could be distributed. Only the lowest Cl_2^{2+} states of each symmetry have been treated in this AO basis. The total SCF energy for the $X\,^1\Sigma_g^+$ ground state of Cl_2 is $-918.990\,55$ hartrees compared to the value of $-918.919\,71$ hartrees in the standard basis and it is $-917.854\,43$ hartrees for the $X\,^3\Sigma_g^-$ state of Cl_2^{2+}. The corresponding CI data for $X\,^3\Sigma_g^-$ are $E_{\text{MRD}}=-918.2502$ hartrees and $E_{\text{full}}=-918.282$ hartrees. While essentially the same reference set is taken for the calculation with the parent MO's as that required for the first calculation employing $X\,^1\Sigma_g^+$ MO's, an optimized reference set is taken in this case, i.e., only those configurations which contribute more than 0.02%. Hence even though the AO basis is larger, the CI calculations are more compact than in the previous two cases.

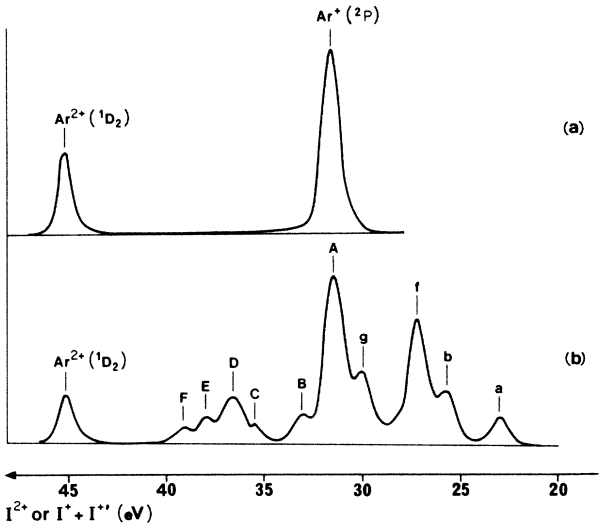

FIG. 2. Translational energy spectra of H^- ions from 3-keV H^+ impinging on (a) Ar and on (b) a mixture of Ar ($\frac{1}{3}$) and chlorine ($\frac{2}{3}$). In both cases the pressure in the collision chamber is 10^{-5} Torr.

EXPERIMENTAL RESULTS

The translational energy spectra of H^- arising from protons colliding with molecular chlorine (99.99% purity from Air Liquide) at rest were recorded with the collision chamber potential floating at a voltage of 100 V. Energy calibration was achieved using argon as a reference gas since the excitation energies involved for single or double charge transfer are comparable with those expected for chlorine. The translational spectrum of the H^- ions recorded for a low pressure of the Ar target gas, i.e., 10^{-5} Torr in the collision chamber and 3×10^{-7} Torr in the apparatus, is reported in Fig. 2(a). The energy difference of 13.4 ± 0.1 eV between the two main peaks is determined by varying the voltage of the ionization source and/or the collision chamber. Absolute ionization energies of 32 and 45 eV were obtained by measuring the voltage across the 127° electrostatic analyzer. An uncertainty of 2 eV is estimated because the trajectory of the ions into the electrostatic analyzer is not well defined. However, the assignment of these two peaks is straightforward. The intensity of the first peak increases with the square of the pressure showing that it is due to a two-step process (see process II) leaving the target in the two sublevels ($^2P_{3/2}$ and/or $^2P_{1/2}$) of the ground state of Ar. Such transitions involve energies $I^+ + I^{+\prime}$ of 31.510, 31.687, and 31.864 eV, respectively, which cannot be resolved with our apparatus. The second peak which has an intensity varying linearly with the pressure is due to a transition into the $^1D_2$ state of Ar^{2+} with a corresponding double ionization potential I^{2+} of 45.112 eV. While absolute double ionization potentials are not accurately measured by this technique, the experimental measurement of 13.4 ± 0.1 eV is in a perfect agreement with the expected difference between I^{2+} and $2I^+$. In the H^- energy distribution there is a small contribution corresponding to the triplet state whose intensity is at least 1 order of magnitude lower than that of $^1D_2$ [see Fig. 2(a)]. This confirms the spin conservation rule already stated.[6,7] The two most intense peaks situated at 31.687 and 45.112 eV are taken as references.

Figure 3 shows two kinetic energy distributions of H^- obtained at two Cl_2 target-gas pressures which differ by a factor of 7, while the pressures measured outside the target cell were, respectively, 10^{-7} and 2×10^{-7} Torr due to the efficiency of the differential pumping. For convenient identification the scale was directly calibrated in terms of ionization energies $I^+ + I^+$ and/or I^{2+}. The spectra were obtained at 0 ± 10^{-3} deg scattering angle. Each spectrum was accumulated over a period of 5 h. The spectra contain 11 narrow peaks between 20 and 40 eV. The ionization energies, the widths, and the relative intensities of these peaks are presented in Tables II and III. Five of them labeled a, b, c, d, and e vary quadratically with the pressure of the target gas and the others A, B, C, D, E, and F vary linearly with pressure.

In order to improve the accuracy of calibration each spectrum for chlorine was preceded and followed by measurement of a spectrum of Ar. Over 60 spectra were taken and the average discrepancy between energies was less than 0.3 eV. The shift was principally due to thermal drift of the high-voltage power supply. The most intense single collision peak (A) appears at an energy of 32.0 eV. To confirm the calibration and to exclude any effects of voltage drift during the runs a spectrum of a mixture of $\frac{1}{3}Ar + \frac{2}{3}Cl_2$ was recorded. The corresponding H^- energy distribution is given in Fig. 2(b) where the peak D is identified as the Ar^{2+} ($^1D_2$) state. Note that the peak ap-

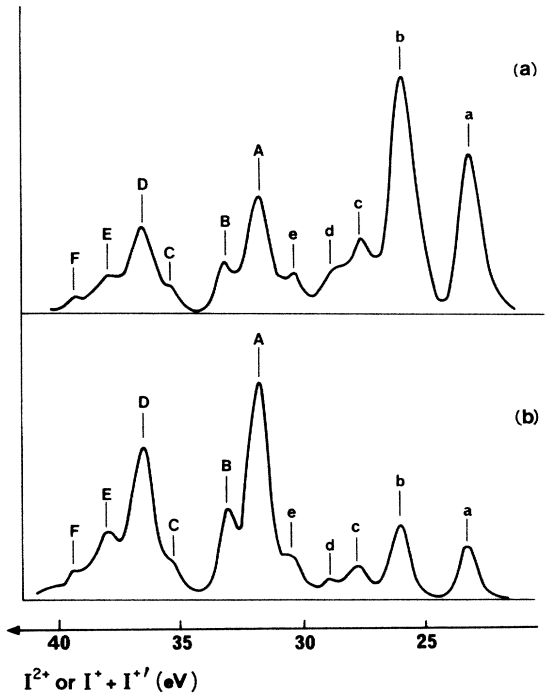

FIG. 3. Translational energy spectra of H^- ions from 3-keV H^+ impinging on (a) Cl_2 at high pressure, (b) Cl_2 at low pressure. The scale is directly calibrated in terms of ionization energies $I^+ + I^{+\prime}$ and/or I^{2+}.

TABLE II. Double-collision processes.

Peak	$I^+(1)+I^+(2)$ experimental value (eV)	Relative height[a]	Width[b] (eV)	Photoelectron spectroscopy[c] (eV)	Discrepancy ΔE (eV)	Attribution
a	23.25±0.2	0.7	0.5	23.12±0.01	0.13	$Cl_2^+(X\,^2\Pi_g)+Cl_2^+(X\,^2\Pi_g)$
b	26.20±0.2	1.0	0.6	25.95±0.01	0.25	$Cl_2^+(X\,^2\Pi_g)+Cl_2(^2\Pi_u)$
c	27.70±0.2	0.2	≃0.5	27.64±0.01	0.06	$Cl_2^+(X\,^2\Pi_g)+Cl_2^+(^2\Sigma_g^+)$
d	28.90±0.2	<0.1		28.79±0.01	0.11	$Cl_2^+(^2\Pi_u)+Cl_2^+(^2\Pi_u)$
e	30.70±0.2	<0.1		30.48±0.01	0.22	$Cl_2^+(^2\Pi_u)+Cl_2^+(^2\Sigma_g^+)$

[a]The most intense peak (b) has been taken as reference.
[b]Measured value after deconvolution.
[c]From Ref. 19.

pearing in the energy range 31.7—32.1 has contributions both from single collision involving Cl_2 and from double collisions with Ar.

The double-collision processes can be interpreted in terms of the photoelectron spectrum of Cl_2.[19] From this study three states $X\,^2\Pi_g$, $A\,^2\Pi_u$, and $B\,^2\Sigma_g^+$ are known to have adiabatic ionization of 11.59, 14.39, and 16.08 eV. Linear combination of two of these three states give six sets of $(I+I^{+\prime})$ values located, respectively, at 23.12, 25.95, 27.64, 28.79, and 30.48 eV. These data permit the identification of all double-collision structures of our spectrum, as shown in Table II. The highest-energy combination ($B\,^2\Sigma_g^+$ twice) is not observed and may be concealed under the first single-collision peak (A). The experimental resolution of the apparatus was estimated to be 0.8 eV from the width of the Ar peaks. Deconvolution of our spectra gives experimental widths for Cl_2^+ states $X\,^2\Pi_g$, $A\,^2\Pi_u$, and $B\,^2\Sigma_g^+$ of 0.3, 0.5, and 0.5 eV in good agreement with previous photoelectron spectroscopy,[19] and this confirms the proposed identification which is given in Table II.

There are only a few reports on differential cross sections[20] in energy and angle in the single charge-exchange processes IIa and IIb. These processes are, however, believed to be most intense at 0° angle scattering, so the heights of the peaks we observe can be estimated to be directly proportional to the cross sections.[20] Within this approximation and from the relative heights of the peaks a, b, and d corresponding to the formation of two Cl_2^+ $(X\,^2\Pi_g)$, $Cl_2^+(X\,^2\Pi_g)+Cl_2^+(A\,^2\Pi_u)$, and two Cl_2^+ in the $A\,^2\Pi_u$ state we can determine the relative cross sections of the processes leading to H production from process IIa:

$$H^+ + Cl_2 \rightarrow \begin{cases} H + Cl_2^+(X\,^2\Pi_g), & \Delta E = -2.0 \text{ eV} \quad [\sigma_1] \\ H + Cl_2^+(^2\Pi_u), & \Delta E = +0.8 \text{ eV} \quad [\sigma_2] \end{cases}$$

and those of two processes forming H^- by process IIb:

$$H + Cl_2 \rightarrow \begin{cases} H^- + Cl_2^+(X\,^2\Pi_g), & \Delta E = +10.7 \text{ eV} \quad [\sigma_{-1}] \\ H^- + Cl_2^+(^2\Pi_u), & \Delta E = +13.8 \text{ eV} \quad [\sigma_{-2}] \,. \end{cases}$$

σ_1 and σ_2 are the cross sections for charge exchanges forming Cl_2^+ ground and excited states, respectively, while σ_{-1} and σ_{-2} refer to formation of the ion pair $Cl_2^+ + H^-$ with Cl_2^+ in the same two states. ΔE is the energy defect corresponding to each reaction. After deconvolution of the experimental data we have deduced the values of the ratios σ_2/σ_1 and σ_{-2}/σ_{-1} as 1.3 and 0.1. The difference of more than a factor of 10 between them is striking, and so far we have been unable to explain it in any straightforward way. We hope that an explanation may eventually be forthcoming from the theory of collisions. Similar conclusions can be drawn from Fig. 2(b) where the Ar + Cl_2 spectrum is reported. Each peak is identified by the energy-loss measurement and we note that the peak f corresponding to the transition into

TABLE III. Double-charge-transfer processes.

Peak	I^{2+} (eV) Experimental value	Relative[a] height	Width[b] (eV)	I^{2+} (eV) Calculated value	ΔE (eV)	Cl_2^{2+} molecular states proposed attribution
				31.24±0.3	0.76	$1\,^1\Delta_g$
A	32.00±0.2	1.0	0.4	31.58±0.3	0.42	$1\,^1\Sigma_g^+$
B	33.10±0.3	0.3	0.3	32.50±0.3	0.60	$1\,^1\Sigma_u^-$
C	35.50±0.4	0.05		34.79±0.3	0.71	$1\,^1\Pi_u$
D	36.60±0.2	0.7	≃0.4	36.07±0.3	0.53	$1\,^1\Delta_u$
E	37.80±0.3	<0.27	≃0.4	37.63±0.3	0.17	$1\,^1\Sigma_u^+$
F	39.20±0.3	<0.16	>0.7	39.15±0.3	0.05	$2\,^1\Sigma_u^-$
				39.38±0.3	0.18	$2\,^1\Pi_u$

[a]The most intense peak (A) has been taken as reference.
[b]Measured value after deconvolution.

$Ar^+ + Cl_2^+(X\,^2\Pi_g)$ is much higher than the peak g corresponding to the transition $Ar^+ + Cl_2^+(A\,^2\Pi_u)$. A good understanding of these reactions will require further investigations using an apparatus having two collision cells so that the individual contributions of the primary and secondary collisions can be effectively separated.

Peaks B, C, D, E, and F have intensities varying linearly with the target pressure. Under the experimental conditions reported in Fig. 2 peak A has a negligible double-collision contribution of a few percent (see the discussion above). All these peaks appearing between 32 and 40 eV must be attributed to electronic transitions into states of the doubly charged ion Cl_2^{2+}. Taking into account the experimental resolution of the apparatus of 0.8 eV, we can deduce the widths of the electronic states reached during the collision, and the corresponding values are given in Table III.

THEORETICAL RESULTS

The computed potential energy curves for Cl_2^{2+} obtained in the standard AO and $X\,^1\Sigma_g^+$ MO basis are contained in Fig. 4. The order of low-lying states is similar to those in isovalent O_2: the π_g^2 states $X\,^3\Sigma_g^-$, $a\,^1\Delta_g$, and $b\,^1\Sigma_g^+$ are followed in the main by the $\pi \rightarrow \pi^*$ excitation states of $\sigma_g^2\pi_u^3\pi_g^3$ configurations $c\,^1\Sigma_u^-$, $A\,^3\Delta_u$, $A\,^3\Sigma_u^-$, $B\,^3\Sigma_u^-$, $^1\Delta_u$, and $^1\Sigma_u^+$, all of which show potential minima

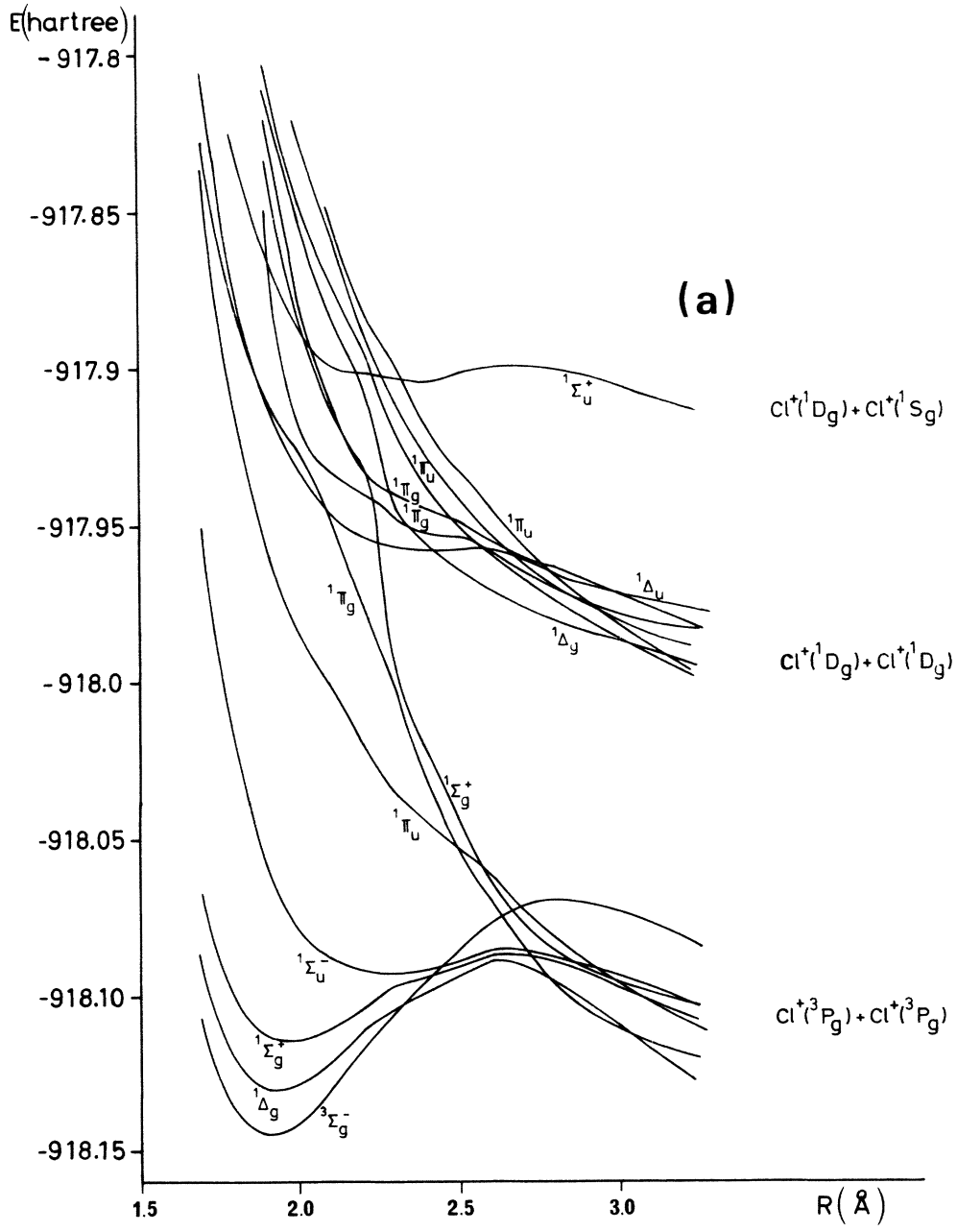

FIG. 4. (a) Calculated potential curves for singlet Cl_2^{2+} states. (b) Calculated potential curves for triplet Cl_2^{2+} states.

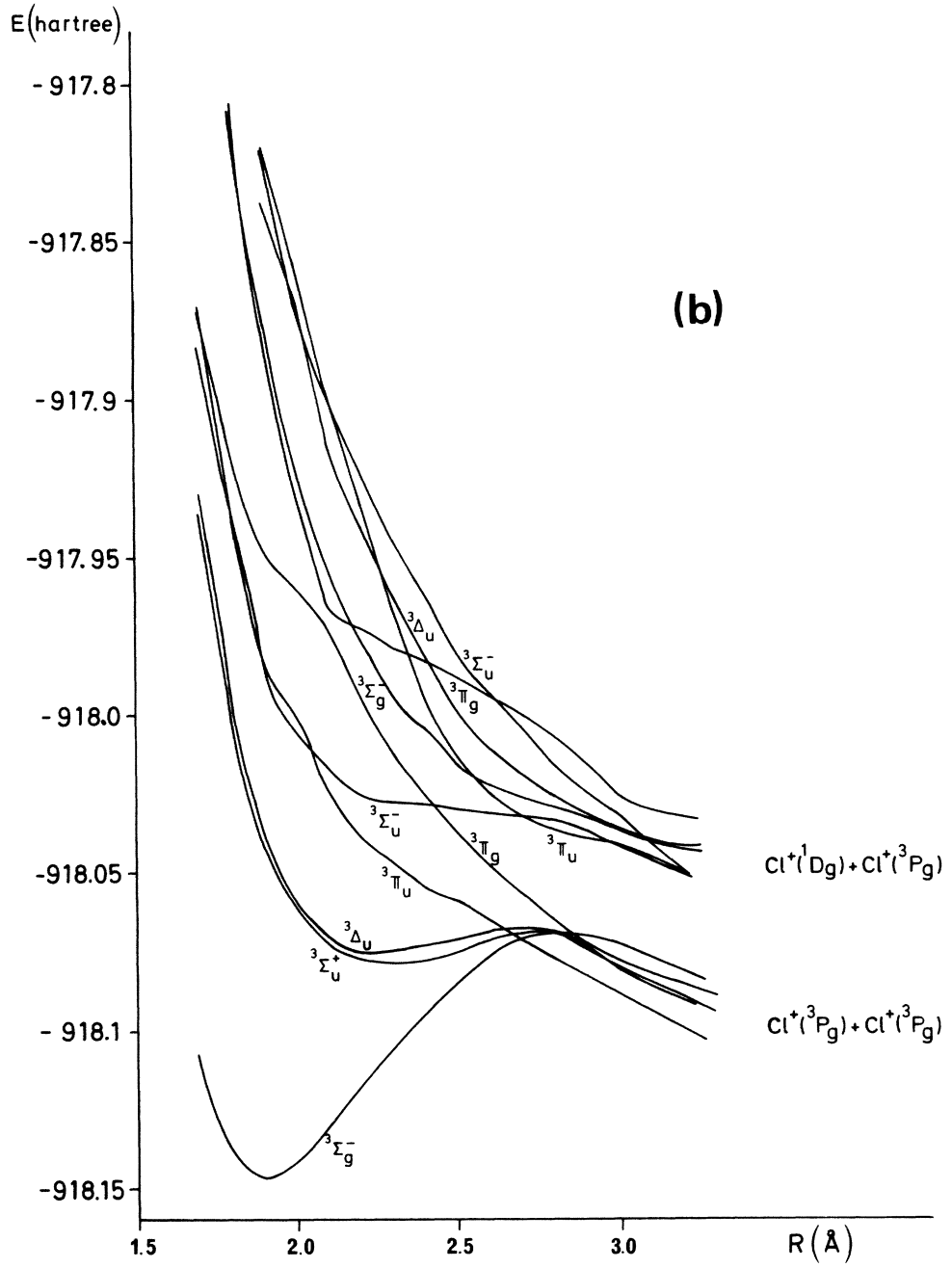

FIG. 4. (*Continued*).

just as in O_2. In addition there are the repulsive Π_u and Π_g states populating either the strongly repulsive σ_u or resulting from $\sigma_g \rightarrow \sigma_g$ transition. The splitting between the π_g^2 states $X\,^3\Sigma_g^-$, $^1\Delta_g$, and $^1\Sigma_g^+$ (Table IV) is somewhat smaller than in O_2 because of the more diffuse charge distribution in Cl_2^{2+} relative to the first-row analogue. In a similar way the higher stability relative to π_u in Cl_2^{2+} and the smaller gap between bonding and antibonding MO's in Cl_2^{2+} in comparison to those of O_2 manifests itself in the relative position of Π_u,Π_g and π_u^3,π_g^3 states, but this behavior is not of great concern in the present study.

In contrast to the potential curves in O_2 all curves are repulsive at large internuclear separations, a finding which has already been pointed out in the early work of Hurley.[11] The $X\,^3\Sigma_g^-$ Cl_2^{2+} minimum is calculated at -918.194 hartrees, i.e., 29.44 eV above the ground-state $X\,^1\Sigma_g^+$ Cl_2^{2+} minimum. The first dissociation limit indicated in Fig. 4 for $^3P+{}^3P$ is found for the various states treated at an internuclear separation of 10 Å between 26.3 and 26.8 eV in reasonable agreement with the observed $^3P(Cl^+)+{}^3P(Cl^+)$ limit at 26.0 eV above the asymptote for $Cl(^2P)+Cl(^2P)$. A similar accuracy is obtained for the two other outgoing channels $^3P_g+{}^1D_g$ and $^1S_g+{}^1D_g$.

All calculated excitation energies are contained in Table IV. It is seen that the results are fairly stable with relatively minor changes between the two different AO basis

TABLE IV. Vertical excitation energies (in eV) obtained for the Cl_2^{2+} states for the three different calculations at $R = 2.0$ Å (see also Table I).

State	Excitation	Standard treatment[a,b]	Parent MO treatment[a,b]	Larger AO basis[a,b]
$X\,^1\Sigma_g^+$ Cl_2	$\sigma_g^2\pi_u^4\pi_g^4$	0.0	0.0	0.0
$X\,^2\Pi_g$ Cl_2^+	$\sigma_g^2\pi_u^4\pi_g^3$	11.934	11.934	11.36
$X\,^3\Sigma_g^-$ Cl_2^{2+}	$\sigma_g^2\pi_u^4\pi_g^2$	30.88	30.583	30.61
$^1\Delta_g$	$\sigma_g^2\pi_u^4\pi_g^2$	31.23	31.163	31.24
$^1\Sigma_g^+$	$\sigma_g^2\pi_u^4\pi_g^2$	31.61	31.537	31.58
$^1\Sigma_u^-$	$\sigma_g^2\pi_u^3\pi_g^3$	32.52	32.50	32.50
$^3\Delta_u$	$\sigma_g^2\pi_u^3\pi_g^3$	32.78	32.702	32.73[b]
		(33.05)[b]	(32.83)[b]	(32.66)
$^3\Sigma_u^+$	$\sigma_g^2\pi_u^3\pi_g^3$	33.03	32.713	32.65
$^3\Pi_u$	$\pi_u^4\pi_g^3\sigma_u$	34.52	33.970	34.05
$^3\Sigma_u^-$	$\sigma_g^2\pi_u^3\pi_g^3$	34.57	34.330	34.48
$^1\Pi_u$	$\sigma_g^2\pi_g\pi_u^4\sigma_u$	35.13	34.812	34.79
$^3\Pi_g$	$\sigma_g^2\pi_u^3\pi_g^2\sigma_u$	35.81	35.346	35.38
$^3\Pi_g$	$\pi_u^4\pi_g^3\sigma_g$	36.60	35.977	35.83
$^1\Delta_u$	$\sigma_g^2\pi_u^3\pi_g^3$	36.61	36.074	36.09
		(36.14)[b]	(36.152)[b]	(36.05)[b]
$^1\Pi_g$	$\pi_u^4\pi_g^3\sigma_g$	36.74	36.440	36.24
$^3\Sigma_g^-$	$\sigma_g^2\pi_u^2\pi_g^4$	36.81	36.525	36.39
$^1\Pi_g$	$\sigma_g^2\pi_u^3\pi_g^2\sigma_u$	36.95	36.557	36.63
$^1\Sigma_u^+$	$\sigma_g^2\pi_u^3\pi_g^3$	37.90	37.577	37.63
$^1\Sigma_g^+$	$\pi_u^4\pi_g^4$	37.96	37.794	
$^1\Pi_g$	$\sigma_g^2\pi_u^3\pi_g^2\sigma_u$	38.03	37.831	
$^3\Pi_u$	$\sigma_g^2\pi_u^2\pi_g^3\sigma_u$	38.24	37.825	38.68
$^3\Delta_u$	$\sigma_g^2\pi_u^3\pi_g^3$	38.27	38.068	38.01
$^3\Sigma_u^-$	$\sigma_g\pi_u^4\pi_g^2\sigma_u$	38.75	38.456	
$^1\Delta_g$	$\pi_u^4\pi_g^4$	38.75	38.172	
$^1\Pi_u$	$\sigma_g\pi_u^3\pi_g^4$	38.86	38.986	39.38
$^1\Sigma_u^-$	$\sigma_g\pi_u^4\pi_g^2\sigma_u$	39.47	39.280	39.15
$^1\Pi_u$	$\sigma_g\pi_u^3\pi_g^4\sigma_u$	40.54	39.821	

[a]For a description of the treatment refer to Table I.

[b]If two numbers are given the first one refers to the Δ component obtained from the $^3B_{3u}$, the other stems from the ^1A_u irreducible representation Hamiltonian matrix.

sets. Larger errors exist if the $X\,^1\Sigma_g^+$ MO's as in the standard treatment are employed, but as stated earlier, this fact is not surprising since the parent MO's give a more appropriate description of the charge distribution.

DISCUSSION

Experimental and theoretical values of doubly charged states of chlorine are reported in Tables III and IV, respectively. The two first singlet states are too close to be distinguished with our experimental resolution. The mean calculated value of 31.4 is 0.6 eV lower than the first experimental state of 32.0 eV. We notice that there is also a systematic deviation of about 0.6 eV between the two following calculated and experimental results. Although this deviation is outside the estimated margin of error, the identification of most of the observed peaks with calculated singlet states can be made in spite of it. It is already well known that theoretical calculations give differences between energy levels with better accuracy than the absolute energies. In Fig. 5 the energy differences between doubly charged states, the proposed assignment in terms of the theoretical calculation, and the previous experimental results[9,10] are all demonstrated.

The first experimental peak found at 32.0 eV is in good agreement with the double ionization appearance potential of 32.6 eV reported in Ref. 9. The discrepancy of 0.6 eV could easily be explained by the difficulty of extrapolating correctly to the true ionization threshold in electron impact, even if electron impact populates the same states as double charge transfer.[21] This peak is the most intense and is attributed to transition to low vibrational levels of the two lowest singlets $1\,^1\Delta_g$ and $1\,^1\Sigma_g^+$. The peak is narrow and the measured experimental width fits well with the width of the corresponding Franck-Condon (FC) zone deduced from the potential curves of Fig. 4 together with the energy difference of 0.3 eV obtained by the calculation for these two states.

The second peak is weaker and appears at 33.1 eV. It corresponds to the high vibrational levels of the $1\,^1\Sigma_u^-$ state which is calculated at 32.5 eV. This transition is forbidden according to the $\Sigma^+ \not\leftrightarrow \Sigma^-$ selection rule;[6] nevertheless, the observation of a weak peak can be explained by the fact that the flat part of the potential curve is located in the FC region of Cl_2. The shape of the calculated curve indicates that dissociation through tunneling

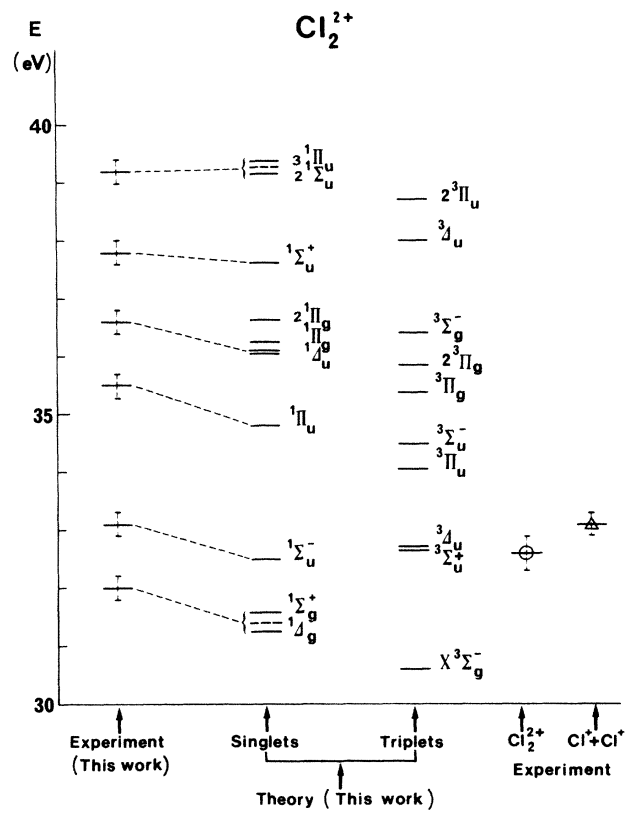

FIG. 5. Comparison between calculated and experimental energies of Cl_2^{2+} electronic states. The theoretical values used correspond to the "larger AO basis" of Table IV and experimental results of this work and of the work of Refs. 9 (○) and 10 (△).

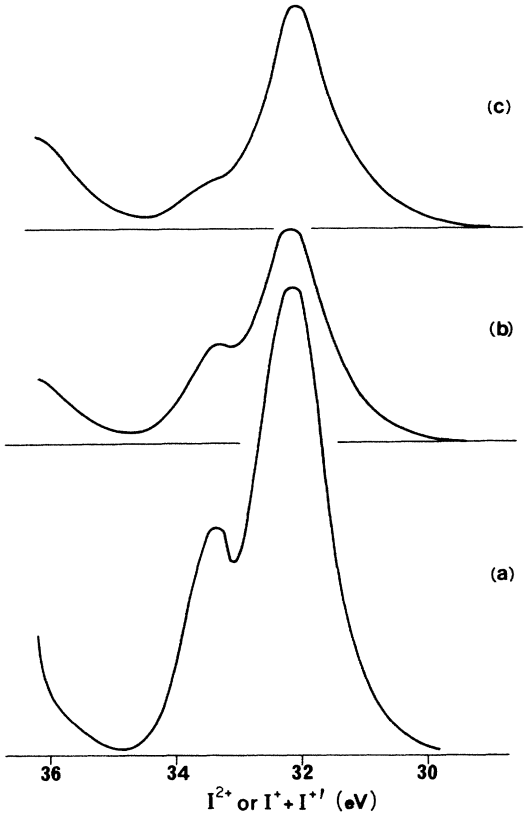

FIG. 6. Spectra of H^- ions corresponding to transitions leading to the formation of Cl_2^{2+} in $1\,^1\Delta_g$ and $1\,^1\Sigma_g^+$ (peak A) and $1\,^1\Sigma_u^-$ (peak B) states for different scattering angles estimated at (a) $\theta=0°$, (b) $\theta=0.1°$, and (c) $\theta=0.2°\pm10^{-3}$.

effect is to be expected. This is supported by the result of Beynon *et al.*[10] who studied the energy released upon the dissociation of Cl_2^{2+} into two singly charged atoms. Adding the measured 4.79-eV energy release to the first dissociation limit of Cl_2^{2+} into $Cl^+(^3P_2)+Cl^+(^3P_2)$ shows that if ground-state products are formed, the electronic state reached by direct excitation following electron impact in their ion source must be located at 33.1 eV, in excellent agreement with the value observed in our experiment. The very close agreement within experimental error strongly suggests that the same state of Cl_2^{2+} is populated in both experiments (their measurements have an uncertainty less than 0.1 eV). These two experimental values confirm the existence of two stable or metastable states of Cl_2^{2+} and confirm also the assumption that theoretical energies are underestimated.

The next allowed state $1\,^1\Pi_u$ is located at 34.79 eV according to the calculation and it appears as a very weak peak (C) at about 35.5 eV in our experiments. Its apparent weakness is explained by the fact that this state is purely dissociative, with a very steep potential energy curve, so the peak is expected to be broad. It is partly overlapped by the tail of the adjacent intense peak D and its width is more than 1 eV as predicted (Fig. 4), so it is difficult to determine its energetic position with good accuracy.

In the experimental results there is a gap in the range of energy between 33.7 and 35.5 eV where all the calculated states are triplets. This is particularly true for the $^3\Sigma_u^-$ state which has a deep well around 2.1 Å and consequently good Franck-Condon factors. This confirms that the spin conservation rule $\Delta S=0$ is obeyed as expected in view of the low spin-orbit coupling constant of Cl_2. This is the reason why we neglect the Cl_2^{2+} ground state ($X\,^3\Sigma_g^-$) in the discussion of the first observed peak (A). The differential cross section for the transitions $Cl_2(X\,^1\Sigma_g^+)\rightarrow Cl_2^{2+}(^1\Delta_g, ^1\Sigma_g^+)$ and $Cl_2(X\,^1\Sigma_g^+)\rightarrow Cl_2^{2+}(^1\Sigma_u^-)$ at different scattering angles of 0°, 0.1°, and 0.2° are reported in Fig. 6. These spectra show clearly that peak B decreases more rapidly with θ than peak A. In an earlier work, Durup[7] has shown that $\Sigma^+\leftrightarrow\Sigma^-$ transitions in atom-diatom collision should have zero cross section at zero scattering angle and the cross sections should behave as $\sin^2\theta$ for small scattering angles. He points out that such transitions are nevertheless relatively favorable in charge-exchange processes. However, experiments on the forward scattering of He in 2.3-keV collisions with N_2 (Ref. 22) showed that the cross section of the $\Sigma^+\leftrightarrow\Sigma^-$ transition is not in fact small in that case compared with the other cross sections. Our result also demonstrates nonvanishing of the transition in double charge exchange but only at 0° scattering angle, and that $\Sigma^+\leftrightarrow\Sigma^-$ transitions are forbidden for nonzero scattering collisions.

The intense peak D located at 36.6 eV is assigned principally to the contribution of the singlet state $1\,^1\Delta_u$ with possible contributions from $1\,^1\Pi_g$ and $2\,^1\Pi_g$. Excitation of the $1\,^1\Delta_u$ state is partly allowed and may fall on the flat (stable) part of its potential curve in the FC region. The two other states are also partly allowed but are dissociative, and would be expected to produce broad weaker peaks; we cannot exclude their making a small contribution to the tail of peak D.

Peak E is weak and appears at 37.8 eV. It is attributed mainly to the transition into the $1\,^1\Sigma_u^+$ state which is the single stable state in this region and fully allowed by the selection rules. All the other singlet states situated in this range of energies are purely dissociative states giving a negligible contribution to the observed peak.

The last peak observed at 39.2 eV is weak and is provisionally attributed to the singlet states $2\,^1\Sigma_u^-$ and $3\,^1\Pi_u$ which are both repulsive. Excitation of the former state is contrary to the $\Sigma^+ \leftrightarrow \Sigma^-$ selection rule. Furthermore, not all the states situated in this range of energies have been calculated. For those two last peaks the agreement between calculated and experimental values seems good, but this agreement may be accidental and the attribution must be considered rather uncertain.

CONCLUSION

The good agreement observed between the results of the calculations and experimental spectrum clearly indicates that the spectral assignments made in the text are basically correct. The match to within 0.6 eV obtained between experimental and calculated vertical energies of Cl_2^{2+} relative to Cl_2 in the vertical Franck-Condon region is well with the accuracy to be expected of the MRD-CI calculations. The observations confirm the spin selection rule, as the triplet states of Cl_2^{2+} are not observed. The symmetry-based selection rules thought to apply to double charge transfer, on the other hand, are not found to be strictly observed.[22]

The good agreement between energies of Cl_2^{2+} states observed here by double charge transfer and earlier measurements using electron impact suggests that the latter process also populates some singlet states of doubly charged ions.

ACKNOWLEDGMENTS

The calculations have been carried out at the Computer Center of the University of Bonn whose services are gratefully acknowledged. This research was supported by the Centre National de la Recherche Scientifique, the Université Paris—Sud, Unité No. 400033 de Recherche. We acknowledge M. Delage from Microcontrole. F.S. wishes to acknowledge a grant from "Fondation de France."

[1]P. Millie, I. Nenner, P. Archirel, P. Lablanquie, P. G. Fournier, and J. H. D. Eland, J. Chem. Phys. **84**, 1259 (1986).

[2]H. Agren, J. Chem. Phys. **75**, 1267 (1981).

[3]D. M. Curtis and J. H. D. Eland, Int. J. Mass Spectrom. Ion Phys. **63**, 241 (1985).

[4]T. Ast, C. J. Porter, C. J. Proctor, and J. H. Beynon, Chem. Phys. Lett. **78**, 439 (1981).

[5]P. G. Fournier, J. Fournier, F. Salama, R. J. Richardson, and J. H. D. Eland, J. Chem. Phys. **83**, 241 (1985).

[6]J. Appell, J. Durup, F. C. Fehsenfeld, and P. G. Fournier, J. Phys. B **6**, 197 (1973).

[7]J. Durup, Chem. Phys. **2**, 226 (1973).

[8]P. G. Fournier, C. Benoit, J. Durup, and R. E. March, C. R. Acad. Sci. B **278**, 1039 (1974).

[9]J. T. Herron and V. H. Dibeler, J. Chem. Phys. **32**, 1884 (1960).

[10]J. H. Beynon, R. M. Caprioli, and J. W. Richardson, J. Am. Chem. Soc. **93**, 1852 (1971).

[11]A. C. Hurley and V. W. Maslen, J. Chem. Phys. **34**, 1919 (1961).

[12]A. Van de Wijngaarden, J. Patel, K. Becker, and G. W. F. Drake, Phys. Rev. A **32**, 2150 (1985), and references therein.

[13]R. J. Buenker and S. D. Peyerimhoff, in *New Horizons of Quantum Chemistry*, edited by P. O. Löwdin and B. Pullmann (Reidel, Dordrecht, 1982), p. 183; R. J. Buenker, S. D. Peyerimhoff, and W. Butscher, Mol. Phys. **35**, 771 (1978).

[14]R. J. Buenker and S. D. Peyerimhoff, Theor. Chim Acta (Berlin) **39**, 217 (1975).

[15]S. D. Peyerimhoff and R. J. Buenker, Chem. Phys. **57**, 279 (1981).

[16]R. P. Tuckett and S. D. Peyerimhoff, Chem. Phys. **83**, 203 (1984).

[17]A. D. McLean and G. S. Chandler, J. Chem. Phys. **72**, 5639 (1980).

[18]A. Banichevich, Diplomarbeit, Universität Bonn, 1986.

[19]H. Van Lonk Huyzen and C. A. De Lange, Chem. Phys. **89**, 313 (1984).

[20]T. R. Dinterman and J. B. Delos, Phys. Rev. A **15**, 463 (1977).

[21]J. H. Beynon, R. G. Cooks, K. I. Jennings, and A. J. Ferreira Correira, Int. J. Mass Spectrom. Ion Phys. **18**, 87 (1975).

[22]Y. Sato, M. Kikuchi, and M. Inouye, Phys. Rev. A **25**, 3376 (1982).